

MEASURING THE DISTANCES TO QUASARS AT HIGH REDSHIFTS WITH STRONG LENSING

KAI LIAO¹

¹ School of Science, Wuhan University of Technology, Wuhan 430070, China.
Draft version August 9, 2019

ABSTRACT

Strongly lensed quasars with time-delay measurements are well known to provide the “time-delay distances” $D_{\Delta t} = (1 + z_L)D_L D_S / D_{LS}$ and the angular diameter distances to lens galaxies D_L . These two kinds of distances give stringent constraints on cosmological parameters. In this work, we explore a different use of time-delay observables: Under the assumption of a flat Universe, strong lensing observations can accurately measure the angular diameter distances to sources D_S . The corresponding redshifts of quasars may be up to $z_S \sim 4$ according to the forecast. The high-redshift distances would sample the Hubble diagram between SNe Ia and CMB, cosmological-model-independently providing direct information on the evolution of the nature of our Universe, for example, the dark energy Equation-of-State parameter $w(z)$. We apply our method to the existing lensing system SDSS 1206+4332 and get $D_S = 2388_{-978}^{+2632} Mpc$ at $z_S = 1.789$. We also make a forecast for the era of LSST. The uncertainty of D_S depends on the redshifts of lens and source, the uncertainties of $D_{\Delta t}$ and D_L , and the correlation between $D_{\Delta t}$ and D_L as well. Larger correlation would result in tighter D_S determination.

Subject headings: cosmology: distance scale - gravitational lensing: strong - methods: data analysis

1. INTRODUCTION

In the standard cosmological model, i.e., Λ CDM, the Universe is flat, dominated by cold dark matter and dark energy with Equation-of-State (EoS) parameter $w \equiv -1$ (Frieman et al. 2008). This concordance scenario is able to explain most of the cosmological observations. However, more and more issues have emerged (Moore 1994, 1999; Frieman et al. 2008; Ding et al. 2015). Especially, the Hubble constant (H_0) measurement based on Cepheids and Type Ia Supernovae (SNe) from local Universe (Riess et al. 2019; Freedman 2017) has 4.4σ discrepancy with measurement from Cosmic Microwave Background (CMB) that assumes the Λ CDM model when inferring H_0 (Planck Collaboration 2018). A recent independent determination of the H_0 based on the Tip of the Red Giant Branch (TRGB) seems to reduce the discrepancy (Freedman et al. 2019). The inconsistency problem would either be related with unknown systematic errors or reveal new physics beyond the standard model. Alternative cosmological models were proposed to solve these issues while new problems may be brought in.

Putting aside the models, from the observational perspective, it is crucial to reconstruct the expansion history of the Universe directly and model-independently from the data (Shafieloo et al. 2006; Shafieloo 2007; Clarkson & Zunckel 2010). Cosmology-free calculations can be also seen in (Bernal et al. 2016; Li et al. 2019; Arendse et al. 2019; Denissenya et al. 2018). If we have distances measured at different redshifts z , we can reconstruct the distance-redshift relation $D(z)$, i.e., the Hubble diagram using cosmology-independent methods, for example, the Gaussian process (Shafieloo et al. 2012; Seikel et al. 2012; Yang et al. 2015). In addition, we can also reconstruct other cosmological quantities evolving with redshift, for example, the Hubble expansion rate

$H(z)$, the deceleration parameter $q(z)$ and the dark energy EoS parameter $w(z)$. These would in turn help us understand the issues related with theoretical models. However, the reconstruction is limited by the maximum redshift z_{max} of the data (L’Huillier et al. 2019). Note that current reliable data used to study cosmology are either at low redshifts $z < 2$, for example SNe Ia (Betoule et al. 2014) and the Baryon Acoustic Oscillations (BAO) (Anselmi et al. 2019), or very high redshift $z \sim 1000$, i. e., the CMB (Planck Collaboration 2018). Other cosmological approaches, for example, cosmic chronometers (Chen et al. 2017) and galaxy clusters (Chen & Ratra 2012) are also at low redshifts. Therefore, it is important to get high-redshift data (hereafter we take $z > 2$ as “high-redshift”) to fill up the data desert between the farthest SN Ia and CMB. The Gamma Ray Bursts (GRBs) can be observed up to $z \sim 8$ and may provide the distance measurements (Schaefer 2003; Izzo et al. 2009; Wei 2010). However, they need calibration by SNe Ia at low redshifts which is very uncertain. Issues also exist about the physical motivation of GRBs as standard candles (Wang et al. 2015). Gravitational waves by compact binary stars can also provide luminosity distances as standard sirens (Schutz 1986), however, the measurement uncertainty would increase remarkably at redshift $z > 2$ (Cai & Yang 2017; Zhao & Wen 2018). Recently, quasars at redshifts up to $z \sim 5$ were proposed to measure the luminosity distances with a method based on X-ray and ultraviolet emission (Risaliti & Lusso 2019). The robustness of this method needs to be further confirmed.

Strongly lensed quasars by galaxies are an excellent tool to study astrophysics and cosmology (Treu 2010). The distant AGN with its host galaxy is lensed by the foreground elliptical galaxy, forming multiple images and arcs of the host galaxy. With the measurements of time-delays between these images, the “time-

delay distance” which is a combination of three angular diameter distances $D_{\Delta t} = (1 + z_L)D_L D_S / D_{LS}$ can be determined (Refsdal 1964; Treu & Marshall 2016). It is known to determine the Hubble constant (Refsdal 1964) and other cosmological parameters, for example, the EoS parameter of dark energy (Linder 2011). The H0LiCOW collaboration (Suyu et al. 2017) has constrained H_0 at 2.4% precision level under a flat Λ CDM model and a weaker constraint in w CDM model due to the degeneracy between H_0 and w (Wong et al. 2019; Taubenberger et al. 2019). In addition to $D_{\Delta t}$, the angular diameter distance to lens galaxy (D_L) was proposed to be determined by combining time-delay measurements with lens stellar velocity dispersion measurements (Paraficz & Hjorth 2009; Jee et al. 2015, 2016; Yıldırım et al. 2019). Four lensing systems have been given the robust D_L measurements (Wong et al. 2019). Note that unlike SNe Ia which determine the relative distances, the strong lensing measures the absolute angular diameter distances, with which one can directly establish the Hubble diagram. However, this approach is limited by the relatively low redshifts of the lenses $z < 1.2$ (Jee et al. 2016).

Motivated by acquiring high-redshift data for studying the Universe, we propose a method to measure the distances to quasars based on strong lensing. The source quasars locate at high redshifts up to $z_S \sim 4$. This paper is organised as follows: In Section 2, we introduce the current status of time-delay strong lensing cosmology. In Section 3, we give the idea of measuring the distances to the sources. Then we apply our method to a realistic system SDSS 1206+4332 in Section 4. We also make a forecast for the lensing observations in LSST era in Section 5. Finally, we summarize and make discussions in Section 6.

2. LENSED QUASARS WITH TIME-DELAYS

According to the theory of strong gravitational lensing (Refsdal 1964; Treu 2010; Treu & Marshall 2016; Liao 2019), the arriving time difference (time-delay) between two images of the source measured from Active Galactic Nucleus (AGN) light curves is related with the geometry of the Universe and the gravity field of lens galaxy through:

$$\Delta t = \frac{D_{\Delta t}}{c} \Delta\phi(\boldsymbol{\xi}_{lens}), \quad (1)$$

where c is the light speed. $\Delta\phi = [(\boldsymbol{\theta}_A - \boldsymbol{\beta})^2/2 - \psi(\boldsymbol{\theta}_A) - (\boldsymbol{\theta}_B - \boldsymbol{\beta})^2/2 + \psi(\boldsymbol{\theta}_B)]$ is the Fermat potential difference between image A and image B. $\boldsymbol{\theta}_A$ and $\boldsymbol{\theta}_B$ are angular positions of the images. $\boldsymbol{\beta}$ denotes the source angular position. ψ is the two-dimensional lensing potential determined by the Poisson equation $\nabla^2\psi = 2\kappa$, where the surface mass density of the lens κ is in units of critical density $\Sigma_{crit} = c^2 D_S / (4\pi G D_L D_{LS})$. $\Delta\phi$ is determined by the lens model parameters $\boldsymbol{\xi}_{lens}$ which can be inferred with high resolution imaging data. $D_{\Delta t}$ is the “time-delay distance” consisting of three angular diameter distances:

$$D_{\Delta t} = (1 + z_L) \frac{D_L D_S}{D_{LS}}, \quad (2)$$

where L, S stands for lens and source. Note that the line-of-sight (LOS) mass structure could also affect time-delay

distance measurements (Falco et al. 1985; Rusu et al. 2017).

At the same time, the angular diameter distance ratio can be measured in a general form (not limited to a Singular Isothermal Sphere (SIS) model as one usually takes):

$$\frac{D_{LS}}{D_S} = \frac{c^2 J(\boldsymbol{\xi}_{lens}, \boldsymbol{\xi}_{light}, \beta_{ani})}{(\sigma^P)^2}, \quad (3)$$

where σ^P is the LOS projected stellar velocity dispersion of the lens galaxy which provides extra constraints to the cosmographic inference. The parameter J captures all the model components computed from angles measured on the sky (the imaging) and the stellar orbital anisotropy distribution. It can be written as a function of lens model parameters $\boldsymbol{\xi}_{lens}$, the light profile parameters $\boldsymbol{\xi}_{light}$ and the anisotropy distribution of the stellar orbits β_{ani} .

Combining Eq.1 and Eq.3, the angular diameter distance to the lens can be measured by:

$$D_L = \frac{1}{1 + z_L} \frac{c\Delta t}{\Delta\phi(\boldsymbol{\xi}_{lens})} \frac{c^2 J(\boldsymbol{\xi}_{lens}, \boldsymbol{\xi}_{light}, \beta_{ani})}{(\sigma^P)^2}. \quad (4)$$

Note that the lensing analysis is quite complicated and we only show the key equations. For dealing with the real data, one should use a full Bayesian analysis considering covariances between quantities to calculate the posteriors of each parameter. We refer to Jee et al. (2015), Shajib et al. (2018), Birrer et al. (2019) and Yıldırım et al. (2019) for more details of such process.

Therefore, the lensed quasars with time-delays could constrain parameters in cosmological models through the measured $D_{\Delta t}$ and D_L . The H0LiCOW project (Suyu et al. 2017) in collaboration with the COSMOGRAIL programme (Courbin et al. 2018) has assembled a sample of lensed quasar systems, six of which (B1608+656, RXJ1131-1231, HE 0435-1223, SDSS 1206+4332, WFI2033-4723, PG 1115+080) have been well-analyzed in the milestone paper (Wong et al. 2019). Among them, four systems have both $D_{\Delta t}$ and D_L measurements. Currently, the H0LiCOW team has only published the posteriors of both $D_{\Delta t}$ and D_L measurements for SDSS 1206+4332. Assuming a flat Λ CDM and through a blind analysis, they reported $H_0 = 73.3^{+1.7}_{-1.8} \text{ km/s/Mpc}$, a 2.4% precision including systematics. A detailed results in different models can be found in (Wong et al. 2019). The previous results from only 4 systems can be found in (Taubenberger et al. 2019).

3. DISTANCES TO THE SOURCES

We propose in this work that strong lensing can also provide the angular diameter distances to quasars (D_S). As long as one assumes the Universe is flat, the three relevant angular diameter distances can be respectively expressed as:

$$D_L = \frac{c}{(1 + z_L)H_0} \int_0^{z_L} \frac{1}{E(z)} dz, \quad (5)$$

$$D_S = \frac{c}{(1 + z_S)H_0} \int_0^{z_S} \frac{1}{E(z)} dz, \quad (6)$$

and

$$D_{LS} = \frac{c}{(1+z_S)H_0} \int_{z_L}^{z_S} \frac{1}{E(z)} dz = D_S - \frac{1+z_L}{1+z_S} D_L, \quad (7)$$

where $E(z) = H(z)/H_0$. Therefore, with Eq.2, the D_S can be determined by:

$$D_S = \frac{(1+z_L)D_L D_{\Delta t}}{(1+z_S)[D_{\Delta t} - (1+z_L)D_L]}. \quad (8)$$

In other words, if lensing observations give $D_{\Delta t}$ and D_L , one can always measure (infer) D_S equivalently. We emphasize that although determining D_S in this way would not bring any benefits (extra information) for constraining parameters in specific cosmological models, the measured D_S at high-redshifts can be further used in the model-independent reconstruction of the expansion history of the Universe, whereas D_L can be replaced by other low-redshift data, for example, the SNe Ia. When applying Eq.8, one should consider the correlation between $D_{\Delta t}$ and D_L . Actually, from strong lensing observations, only one distance among D_L , D_S and $D_{\Delta t}$ is totally independent. While the community uses either D_L or $D_{\Delta t}$, we focus on D_S in this work. In principle, rather than inferring it from $D_{\Delta t}$ and D_L , one can directly take D_S as the lensing parameter in the first place during the lensing analysis. For example, for the simplest case where the lens is describe by a SIS model (Paraficz & Hjorth 2009), the density distribution is given by:

$$\rho_{SIS}(r) = \frac{\sigma^2}{2\pi G r^2}, \quad (9)$$

where σ^2 is the three-dimensional isotropic velocity dispersion. Then

$$D_{\Delta t} = \frac{2c\Delta t}{\theta_A^2 - \theta_B^2}, \quad (10)$$

and

$$D_L = \frac{c^3 \Delta t}{4\pi\sigma^2(1+z_L)\Delta\theta}. \quad (11)$$

Thus we can directly relate D_S with observations by combining Eq.8, Eq.10 and Eq.11.

While we take the SIS model for illustration purposes, one should note that realistic lenses are much more complicated. Different components in the mass models were explored both for lensing and for kinematics (Jiang & Kochanek 2007; Jee et al. 2015; Shajib et al. 2018a,b). For the macro mass model, one needs to consider more properties for individual lenses, for example, the ellipticity and the density slope. A singular elliptical power-law model may not be sufficient and one usually tries a composite model consisting of a baryonic component linked to the stellar light distribution plus an elliptical NFW dark matter halo. In some cases, the lens is during a merger process, for example, B1608+656 shows two interacting lens galaxies (Suyu et al. 2010). Besides, substructures, for example, the satellites and the dark matter subhalos would make observations anomalous if one ignore them (Liao et al. 2018). Furthermore, the nearby galaxies, the line-of-sight structure can also make the lens modelling complicated.

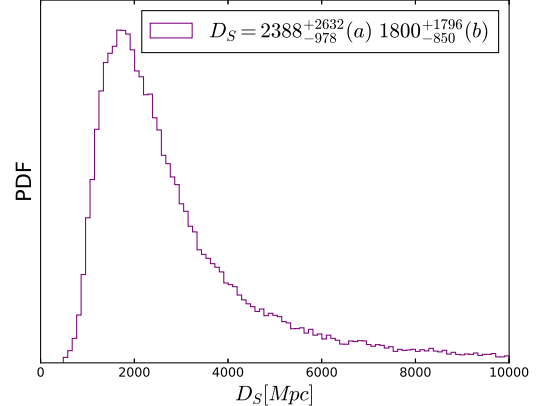


FIG. 1.— Measurement of the distance to the source for SDSS 1206+4332. We adopt two statistics for the distribution: (a) The mean value plus the 16th and 84th percentiles; (b) The most probable value plus 68% probability. The lower and upper limits have the same probability density.

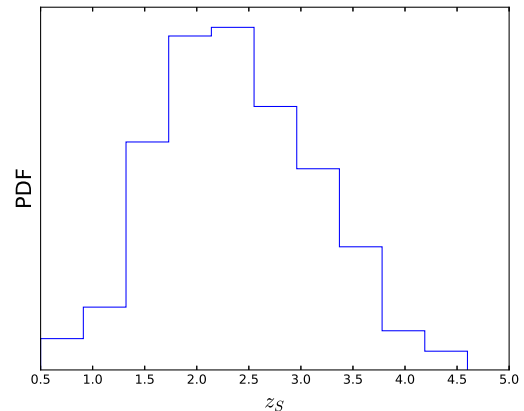


FIG. 2.— The redshift distribution of the sources. 65% of the systems would have $z_S > 2$ resulting 35 high-redshift distance measurements.

4. MEASUREMENT OF SDSS 1206+4332

We apply our method to the system SDSS 1206+4332 which was discovered by (Oguri et al. 2005). It is one of high-quality lensing systems in the catalog of H0LiCOW and has been modeled by (Birrer et al. 2019) within the program. This system consists of a doubly lensed quasar with the host galaxy forming a nearly-complete Einstein ring. The image separation is 3.03'' and the time-delay measured from the light curve pair is 111.3 ± 3 days. The redshifts of lens and source are $z_L = 0.745$ and $z_S = 1.789$, respectively. The H0LiCOW team took a blind time-delay strong lensing cosmographic analysis of the system. They combined the time-delay measurement between the two AGN images, Hubble Space Telescope imaging, spectroscopic data of the lens galaxy and the line-of-sight field measurements to give measurements of both D_L and $D_{\Delta t}$ with systematic errors under control. The two distances are provided on the website¹ of the program in the form of tables of parameters sampled from the posterior distributions. Note the correlation

¹ <http://www.h0licow.org>

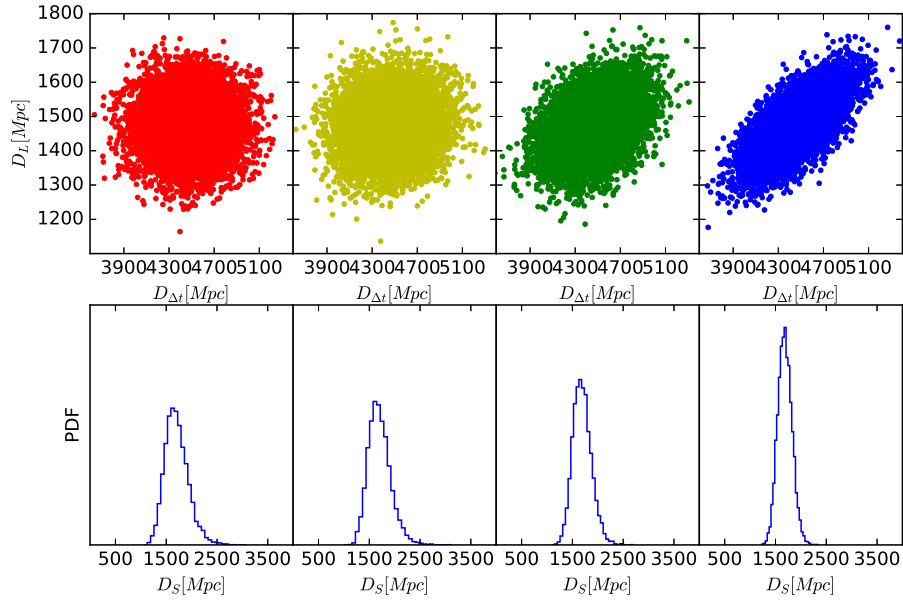


FIG. 3.— A typical case with $z_L = 0.7$ and $z_S = 2.5$. The uncertainties of $D_{\Delta t}$ and D_L are set by 5%. The upper panels show the simulated $D_{\Delta t}$ and D_L distributions with different correlation amplitudes: $\rho = 0, 0.1, 0.4, 0.7$, respectively. The bottom panels are the corresponding D_S inferences.

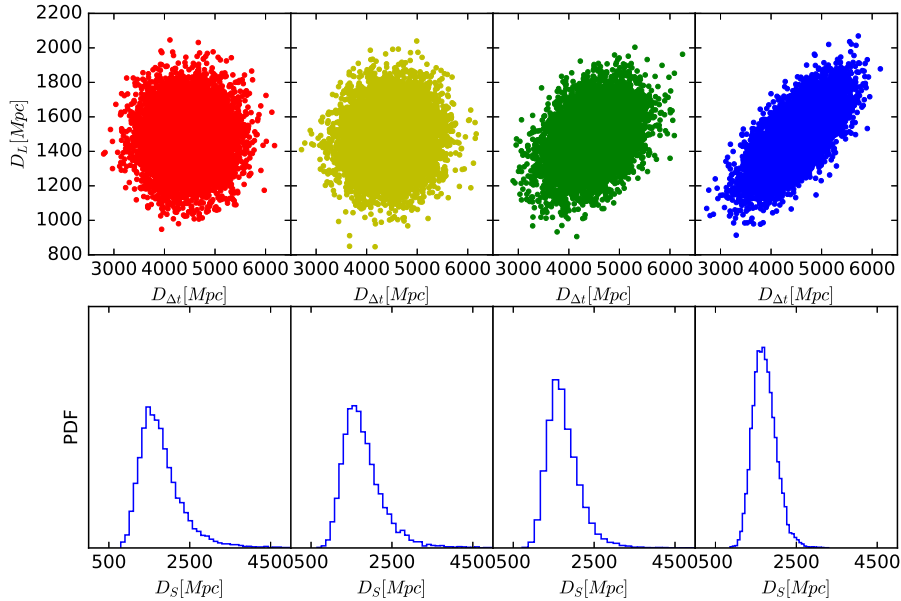


FIG. 4.— The same as Fig.3 but for 10% uncertainties of $D_{\Delta t}$ and D_L .

between them is quite slight with current uncertainties.

For each pair of $(D_{\Delta t}, D_L)$ in the posterior tables, i.e., each point in the two dimensional marginalized distributions of $D_{\Delta t}$ and D_L (see Fig.12 in Birrer et al. 2019), we calculate D_S based on Eq.8 considering the correlation in this way. The distribution of D_S is shown in Fig.1. The median value plus the 16th and 84th percentiles is $D_S = 2388^{+2632}_{-978}$ Mpc. We notice the distribution is very deviated from Guassian-like, therefore, we also give the most probable value $D_S = 1800^{+1796}_{-850}$ Mpc, where the

lower and upper limits have the same probability density and include 68% probability. We approximately fit the distribution in Fig.1 with a log-normal function:

$$P(D_{\Delta t}) = \frac{1}{\sqrt{2\pi}(x - \lambda_D)\sigma_D} \exp\left[-\frac{(\ln(x - \lambda_D) - \mu_D)^2}{2\sigma_D^2}\right], \quad (12)$$

where $x = D_{\Delta t}/(1Mpc)$ and the parameters $(\lambda_D = 1050, \sigma_D = 1.10, \mu_D = 7.43)$.

Note that SDSS 1206+080 is the only doubly lensed system among the current 6 H0LiCOW

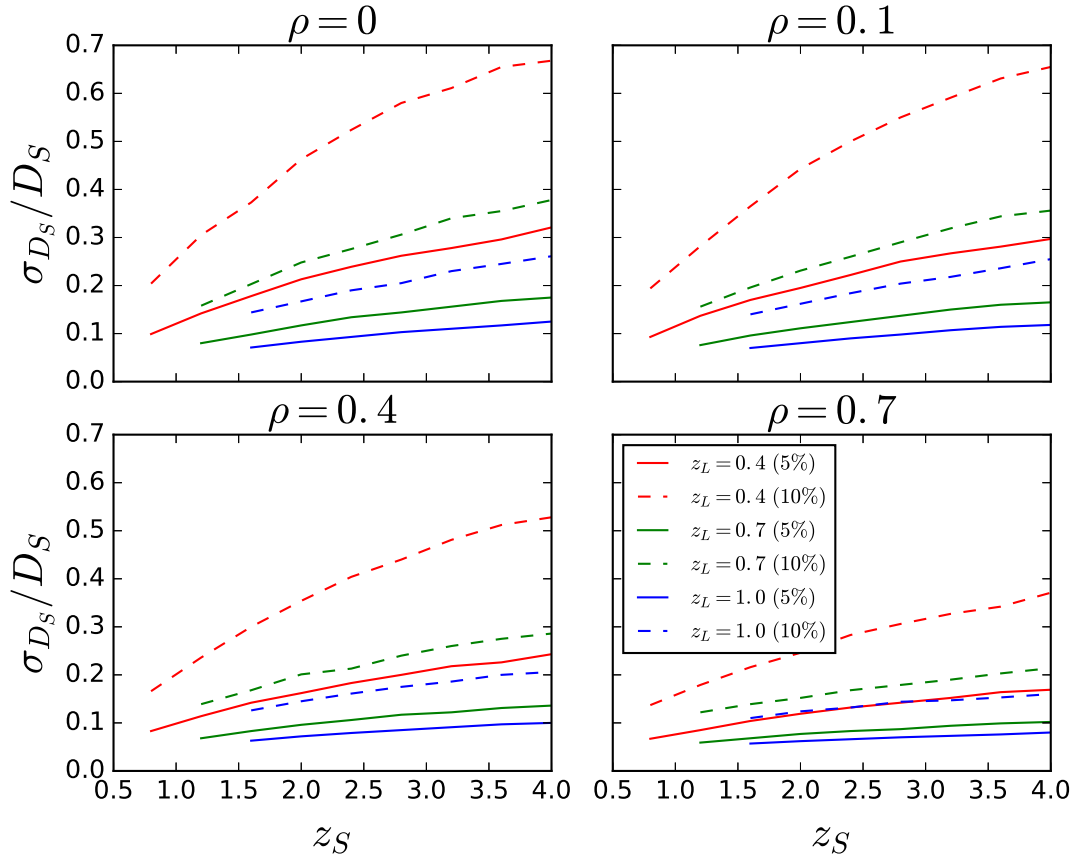


FIG. 5.— The relative uncertainties of the D_S measurements for different lens redshift z_L and source redshift z_S . The precisions of $D_{\Delta t}$ and D_L are taken as 5% and 10% respectively. The impacts of different correlation amplitudes between $D_{\Delta t}$ and D_L are shown in the 4 subfigures, respectively.

lenses (Wong et al. 2019), $D_{\Delta t} = 5769_{-471}^{+589} Mpc$ and $D_L = 1805_{-398}^{+555} Mpc$. The uncertainties of $D_{\Delta t}$ and D_L are $\sim 9\%$ and $\sim 26\%$. For quadruply lensed systems, the uncertainties would be much smaller. For example, $D_{\Delta t}$ is constrained with $\sim 4.3\%$ precision in RXJ1131-12131, and D_L is constrained with $\sim 13\%$ in B1608+656 (Wong et al. 2019).

5. FORECAST IN THE LSST ERA

An increasing number of lensed quasars are being discovered by the current surveys, for example, the Dark Energy Survey (DES) and the Hyper Suprime-Cam Survey (HSC). Moreover, the upcoming Large Synoptic Survey Telescope (LSST) (Oguri & Marshall 2010) will bring us thousands of lensed quasars, some of which will have long-time high-quality light curves for each lensed image. The Time Delay Challenge (TDC) program (Liao et al. 2015) has proved that with good algorithms, there will be ~ 400 well-measured time-delays with average precision $\sim 3\%$ and the average bias $< 1\%$. According to Eq.1 and Eq.3, to obtain the distance information, ancillary data are needed in terms of a few percent measurement of the spatially resolved velocity dispersion of the lens galaxy, the LOS mass fluctuation and the highly resolved imaging from space telescopes. Therefore, as in Jee et al. (2016), we set the following criteria: 1) the AGN image separation should be $> 1''$ to distinguish them; 2) the third brightest image should

be bright enough, its i-band magnitude $m_i < 21$; 3) the lens galaxy should be bright enough $m_i < 22$; 4) quadruply imaged lenses which carry more information to break the Source-Position Transformation (SPT), such that the uncertainty of the lens modelling process is comparable with the time-delay measurements, leading to percent level distance measurements from individual lenses.

With these assumptions, there will be ~ 55 high-quality lenses of the 400 lenses mentioned above selected from the mock LSST catalog (Oguri & Marshall 2010) that can give both $D_{\Delta t}$ and D_L measurements. However, this number may vary due to the real distributions of the lens galaxies and quasars. Besides, the telescope observation strategy also limit the estimate, for example, the spectroscopic follow-up may require brighter lenses, for a shallower limit $m_i < 21$ of the lens galaxies, the number would be only ~ 35 . In the best case, both time-delay measurements and the lens modelling should achieve several percent precision. We take $\sim 5\%$ precision for the distances as in (Jee et al. 2016; Linder 2011). We also consider $\sim 10\%$ precision which is allowed by current techniques for comparison. These lenses will be “blind analysed” that can effectively control the systematic errors which would bias the results. The two dimensional distributions of z_L and z_S can be found in Jee et al. (2016). We marginalize z_L and get the distribution of z_S in Fig.2. As one can see, a large part of the corresponding quasars have high redshifts. ~ 35 systems are with

$z_S > 2$.

To make a forecast, we take a fiducial flat Λ CDM model with $H_0 = 70 \text{ km/s/Mpc}$, $\Omega_M = 0.3$ for the simulation. For each lensing system, given z_L and z_S , we firstly calculate the fiducial values of $D_{\Delta t}$ and D_L , then randomly generate 10000 realizations for each of them. The noise levels follow Gaussian distributions with uncertainties 5% and 10%, respectively. The uncertainties of $D_{\Delta t}$ and D_L primarily come from the external convergence and the velocity dispersion of the lens, respectively. However, since measurements of $D_{\Delta t}$ and D_L are based on the same lens model, one should consider the correlation between them unless one of the distances have much larger uncertainty. According to the simulation by (Yildırım et al. 2019), the correlation is positive. We therefore try different correlation amplitudes for $D_{\Delta t}$ and D_L with correlation coefficients $\rho = 0.1, 0.4, 0.7$, respectively.

Then for each simulated $D_{\Delta t}$ and D_L pair, we calculate D_S based on Eq.8. At last, we get the distribution of D_S along with its median value plus 16th and 84th percentiles. Fig.3 and Fig.4 correspond to a typical case where $z_L = 0.7, z_S = 2.5$ for uncertainties 5% and 10% of $D_{\Delta t}$ and D_L , respectively. We plot the simulated $D_{\Delta t}$ and D_L distributions with different correlations at the upper panels and calculate the corresponding Probability Density Distribution (PDF) of D_S at the bottom panels. One can see the constraint becomes tighter when the correlation is larger. To show the dependence on the redshifts of the lens and source, the uncertainties of $D_{\Delta t}$ and D_L , and the correlation amplitude for the whole samples, we plot Fig. 5 where $\sigma_{D_S} = (84^{\text{th}} \text{percentile} - 16^{\text{th}} \text{percentile})/2$ is taken as an estimate of the uncertainty.

6. SUMMARY AND DISCUSSIONS

In this work, we find another powerful cosmological application of strong gravitational lensing. We propose to measure the angular diameter distances to quasars at high redshifts with strong lensing and apply the method to SDSS 1206+4332. We also explore the power in the future LSST era and give the constraint dependence on the properties of the systems. Rather than constraining a specific cosmological model, distances measured to the sources would benefit reconstructing the nature of the Universe model-independently and directly at high redshifts. A further work will emulate the reconstruc-

tion. Note that the measured high-redshift angular diameter distances can be used to find their maximum value and the corresponding redshift since unlike luminosity distance, angular diameter distance would decrease if the redshift is larger than certain value $z \sim 1.6$ (Salzano et al. 2015).

Very recently, Yıldırım et al. (2019) presented a joint strong lensing and stellar dynamical framework for future time-delay cosmography purposes. With the observations of high signal-to-noise integral field unit (IFU) from the next generation of telescopes, they proved that $D_{\Delta t}$ can be constrained with 2.3% uncertainty and D_L with 1.8% at best for a system like RXJ1131. In such cases, we can acquire much more precise D_S as well, making this idea very promising. Note that RXJ1131 is the best case whereas an ordinary lens system would give larger uncertainties.

Our method relies on the inputs of $D_{\Delta t}$ and D_L measurements by the H0LiCOW-like lensing teams. With more and more precise measurements, the intrinsic (unknown) systematic errors would be quite important. If the $D_{\Delta t}$ and D_L are biased, the inferred D_S would also be biased. The H0LiCOW team has adopted a blind analysis to control systematics. Data challenges, e.g., the Time Delay Challenge (Liao et al. 2015) and the Lens Modelling Challenge (Ding et al. 2018) would reveal the systematics by algorithms. The systematics from unknown physical process would be further revealed by independent approaches. Considering the 5% and 10% uncertainties assumed in this work, a small systematic error, for example, 2% would not bias the results. There are great concerns about the lens modelling systematics being dominated by systematics (Schneider & Sluse 2013; Birrer et al. 2016; Tie & Kochanek 2017). However, the point is no benefit from combining lenses to constrain the cosmological models. In this work, we only focus on determining individual D_S .

7. ACKNOWLEDGMENTS

I thank the anonymous referee for his/her efforts to improve the quality of the paper, and Simon Birrer for introducing the data of SDSS 1206+4332 on the H0LiCOW website. This work was supported by the National Natural Science Foundation of China (NSFC) No. 11603015 and the Fundamental Research Funds for the Central Universities (WUT:2018IB012).

REFERENCES

- Anselmi S., Corasaniti P.-S., Sanchez A. G., et al., 2019, PhRvD, 99, 123515
 Arendse N., Agnello A., Wojtak R., 2019, arXiv: 1905.12000
 Birrer S., Amara A., Refregier A., 2016, JCAP, 08, 020
 Birrer S., Treu T., Rusu C. E., et al., 2019, MNRAS, 484, 4726
 Betoule M., Kessler R., Guy J., et al., 2014, A&A, 568, A22
 Bernal J. L., Verde L., Riess A. G., 2016, JCAP, 10, 019
 Chen Y., Ratra B., 2012, A&A, 543, A104
 Chen Y., Kumar S., Ratra B., 2017, ApJ, 835, 86
 Cai R.-G., Yang T., 2017, PhRvD, 95, 044024
 Clarkson C., Zunckel C., 2010, PhRvL, 104, 211301
 Courbin F., Bonvin V., Buckley-Geer E., et al., 2018, A&A, 609, A71
 Denissenya M., Linder E. V., Shafieloo A., 2018, JCAP, 03, 041
 Ding X., Biesiada M., Cao S., Li Z., Zhu Z.-H., 2015, ApJ, 803, L22
 Ding X., Treu T., Shajib A. J., et al., 2018, arXiv: 1801.01506
 Frieman J. A., Turner M. S., Huterer D., 2008, Annu. Rev. Astro. Astrophys., 46, 385
 Freedman W. L., 2017, Nature Astronomy, 1, 0121
 Freedman W. L., Madore B. F., Hatt D., et al., 2019, arXiv:1907.05922
 Falco E. E., Gorenstein M. V., Shapiro I. I., 1985, ApJ, 289, L1
 Izzo L., Capozziello S., Govone G., Capaccioli M., 2009, A&A, 508, 63
 Jee I., Komatsu E., Suyu S. H., 2015, JCAP, 11, 033
 Jee I., Komatsu E., Suyu S. H., Huterer D., 2016, JCAP, 04, 031
 Jiang G., Kochanek C. S., 2007, ApJ, 671, 1568
 Li E.-K., Du M., Xu L., 2019, arXiv: 1903.11433
 Liao K., Treu T., Marshall P., et al., 2015, ApJ, 800, 11
 Liao K., Ding X., Biesiada M., Fan X.-L., Zhu Z.-H., 2018, ApJ, 867, 69
 Liao K., 2019, ApJ, 871, 113
 Linder E. V., 2011, PhRvD, 84, 123529.

- L'Huillier B., Shafieloo A., Linder E. V., Kim A. G., 2019, MNRAS, 485, 2783
- Moore B., 1994, Nature, 370, 629
- Moore B., Ghigna S., Governato F., et al., 1999, ApJ, 524, L19
- Oguri M., Inada N., Hennawi J. F., et al., 2005, ApJ, 622, 106
- Oguri M., Marshall P. J., 2010, MNRAS, 405, 2579
- Planck Collaboration, 2018, arXiv: 1807.06209
- Paraficz D., Hjorth J., 2009, A&A, 507, L49
- Refsdal S., 1964, MNRAS, 128, 307
- Riess A. G., Casertano S., Yuan W., Macri L. M., Scolnic D., 2019, ApJ, 876, 85
- Rusu C. E., Fassnacht C. D., Sluse D., et al., 2017, MNRAS, 467, 4220
- Risaliti G., Lusso E., 2019, Nature Astronomy, 3, 272
- Schaefer B. E., 2003, ApJ, 583, L67
- Shafieloo A., Alam U., Sahni V., Starobinsky A. A., 2006, MNRAS, 366, 1081
- Shafieloo A., 2007, MNRAS, 380, 1573
- Shafieloo A., Kim A. G., Linder E. V., 2012, PhRvD, 85, 123530
- Seikel M., Clarkson C., Smith M., 2012, JCAP, 06, 026
- Schutz B. F., 1986, Nature, 323, 310
- Shajib A. J., Treu T., Agnello A., 2018a, MNRAS, 473, 210
- Shajib A. J., Birrer S., Treu T., et al., 2018b, MNRAS, 483, 5649
- Suyu S. H., Marshall P. J., Auger M. W., et al., 2010, ApJ, 711, 201
- Suyu S. H., Bonvin V., Courbin F., et al., 2017, MNRAS, 468, 2590
- Salzano V., Dabrowski M. P., Lazkoz R., 2015, PhRvL, 114, 101304
- Schneider P., Sluse D., 2013, A&A, 559, A37
- Treu T., 2010, Annu. Rev. Astron. Astrophys. 48, 87
- Treu T., Marshall P. J., 2016, The Astronomy and Astrophysics Review, 24, 11
- Taubenberger S., Suyu S. H., Komatsu E., 2019, arXiv:1905.12496
- Tie S. S., Kochanek C. S., 2017, MNRAS, 473, 80
- Wei H., 2010, JCAP, 1008, 020
- Wang F. Y., Dai Z. G., Liang E. W., 2015, New Astronomy Reviews, 67, 1
- Wong K. C., Suyu S. H., Chen G. C.-F., et al., 2019, arXiv:1907.04869
- Yang T., Guo Z.-K., Cai R.-G., 2015, PhRvD, 91, 123533
- Yıldırım A., Suyu S. H., Halkola A., 2019, arXiv:1904.07237
- Zhao W., Wen L., 2018, PhRvD, 97, 064031